Ultra high-resolution shallow marine imaging with a sparker over a deep streamer

Vetle Vinje[1], Florian Josse[2], Thibaut Choquer[3], Peng Zhao[1], Isabelle Thauvin[4], Patrick Charron[5] and Philippe Herrmann[2] investigate a novel UHR configuration deployed during a field test in June 2024 offshore Concarneau in France where a deep streamer was towed underneath a new sparker source.

Introduction

Ultra high-resolution (UHR) marine seismic is a scaled-down version of conventional seismic acquisition. Source-receiver separation and depth, shooting rate and seismic wavelengths are typically ten times smaller than for conventional seismic operations. Under ideal conditions, ten times higher subsurface resolution may be achieved, but there will also be less depth penetration due to anelastic damping of the high-frequency seismic waves.

While UHR marine seismic has traditionally been used for geohazard mapping for the oil and gas sector, it has gained popularity in recent years to map boulders, shallow gas and geomechanical properties in the shallow water bottom for offshore windfarm planning. Both 2D and 3D UHR applications have been used (Telling et al., 2024, Davies et al., 2020, Lebedeva-Ivanova et al., 2018)

One common drawback of the typical UHR survey configuration aiming to achieve frequencies above 1000 Hz relates to the shallow tow of the hydrophone streamers (0.5 to 1 m depth). This makes them vulnerable to adverse weather conditions, leading to significant downtime. Furthermore, the signature of sparker sources has notches in their spectra (Kluesner et al., 2019) and the source wavelet is typically not measured directly; making it hard to estimate. In this paper, we will investigate a novel UHR configuration deployed during a field test in June 2024 offshore Concarneau in France where a deep streamer was towed underneath a new sparker source. We will compare images of the shallow geology using this novel source-over-streamer configuration with a traditional UHR configuration where the streamer was towed at a shallow depth behind the source acquired along the same 2D line. Both surveys were processed and imaged by the same group using the same toolbox of technologies.

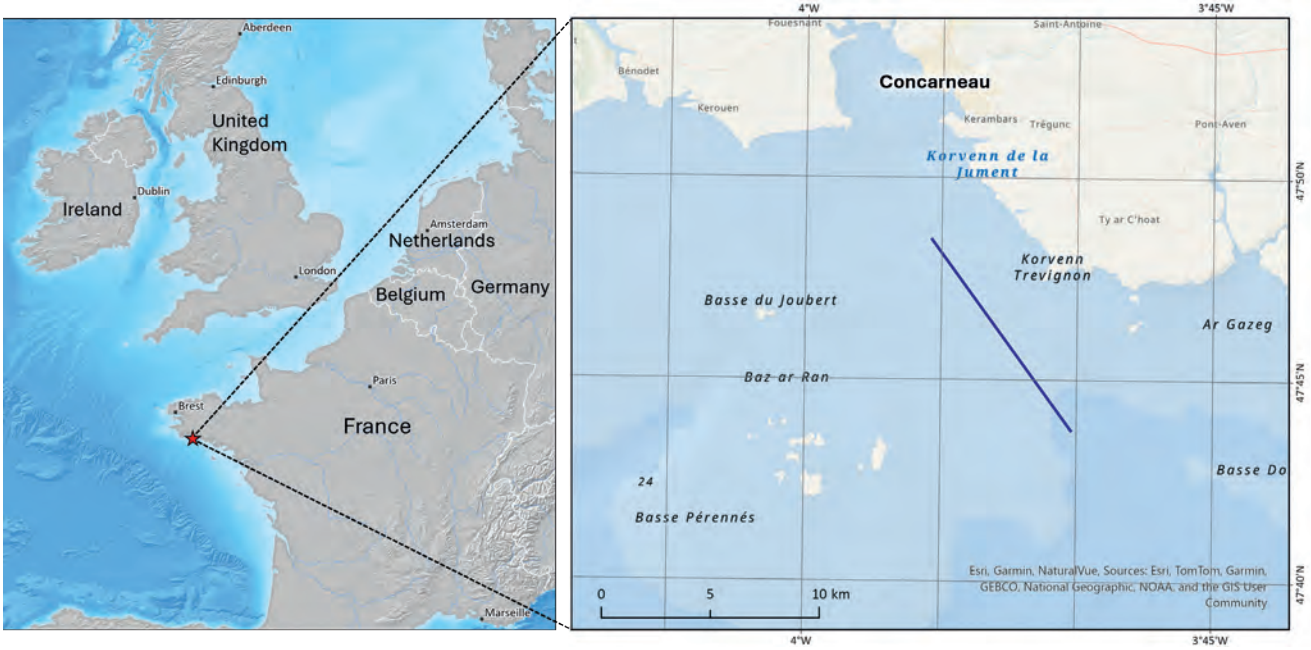

Figure 1 Map of the survey area close to Concarneau with the acquisition line in blue.

[1] Viridien | [2] Sercel (a Viridien Business) | [3] Kappa | [4] SIG | [5] TotalEnergies
* Corresponding author, E-mail: vetle.vinje@viridiengroup.com
DOI: 10.3997/1365-2397.fb2025061

Source type	SIG KappaSpark sparker
Source characteristics	1400 J, 200 tips, single level
Shot spacing	~ 1.8 m
Source depth	~ 0.6 m
Nav system	Sercel Concept Orca
Depth control and recorders	Sercel Nautilus system
Surface positioning system	Fugro Citius RGPS
Streamer type	Sercel UHR streamer
Sensor type	Dual hydrophone array
Streamer length	146.875 m
Number of channels	48
Channel separation	3.125 m
Temporal sampling rate	0.25 ms (2000 Hz nyquist frequency)

Table 1 Common acquisition parameters for the Conventional and Novel test lines.

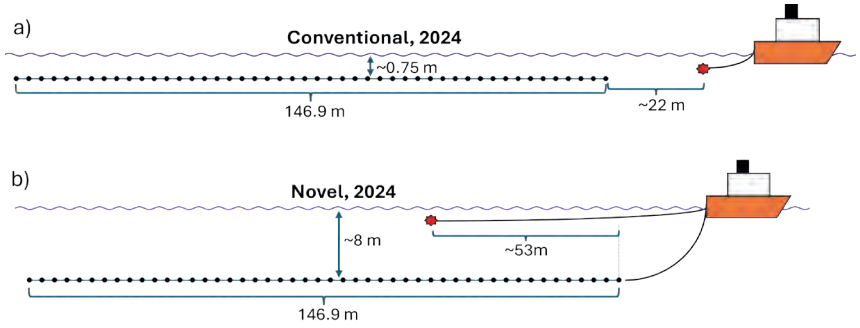

Figure 2 The UHR seismic survey geometries from the field test compared in this study; (a) a conventional acquisition and (b) a source above a deep streamer acquisition.

Seismic surveys offshore Concarneau

The field test was initiated by Sercel, Kappa Offshore, SIG and TotalEnergies and conducted on 19-20 June 2024 offshore Concarneau in Brittany, France (Figure 1).

The geology in the area is formed by a tectonic Eocene depression later draped by late Pleistocene and 3-5 m thick Holocene sediments (Flamme et al., 2020). The Eocene series are faulted and folded, while the upper sedimentary layers are characterised by biogenic gas generated by bacterial activity in the sediments rich in organic material. This gas is present as a multitude of shallow gas pockets and has also outgassed at the seabed, creating myriads of shallow pockmarks that are typically 30 m wide and 2-3 m deep (Dusart et al. 2022).

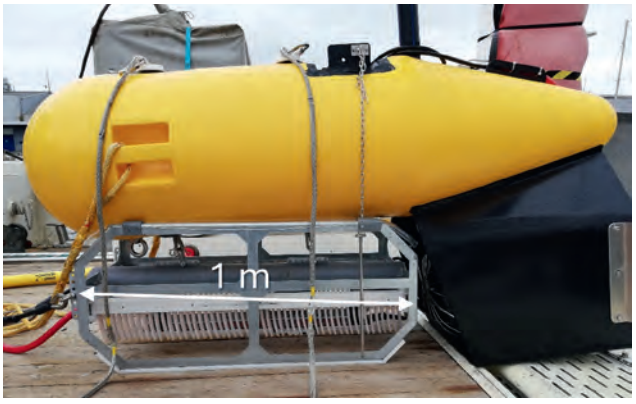

Figure 3 The sparker source used in the Conventional and Novel surveys.

The trajectory of the two straight ~10 km 2D test lines from June 2024 described in this paper is shown as the blue line in Figure 1 and runs over water depths of 30-40 m. We will compare seismic images from two acquisition configurations: (i) a conventional UHR survey geometry with a shallow streamer towed behind the source and (ii) a survey geometry where the source was towed above a deep streamer, as shown in Figure 2a and 2b respectively.

We refer to these as the *Conventional* and *Novel* surveys throughout this paper. They were acquired with the same equipment and the same lateral and temporal sampling, as shown in Table 1.

Although the source-over-spread concept has been successfully applied in conventional seismic in the search for hydrocarbons (Vinje et al., 2017, Camerer et al., 2018), it has not been documented or published for UHR seismic.

In the Novel survey in Figure 2b the source was located directly above the deep streamer at around 8 m in depth. The actual shape of the streamer sagged slightly in the middle with depths varying between 7 and 9 m. Both the Conventional and the Novel tests were run with the same source, the same UHR streamer, and the same spatial and temporal sampling rate, as shown in Table 1.

The sparker source

The sparker used in both surveys is a SIG KappaSpark sparker specifically designed for this field test. The 200 sparker tips were

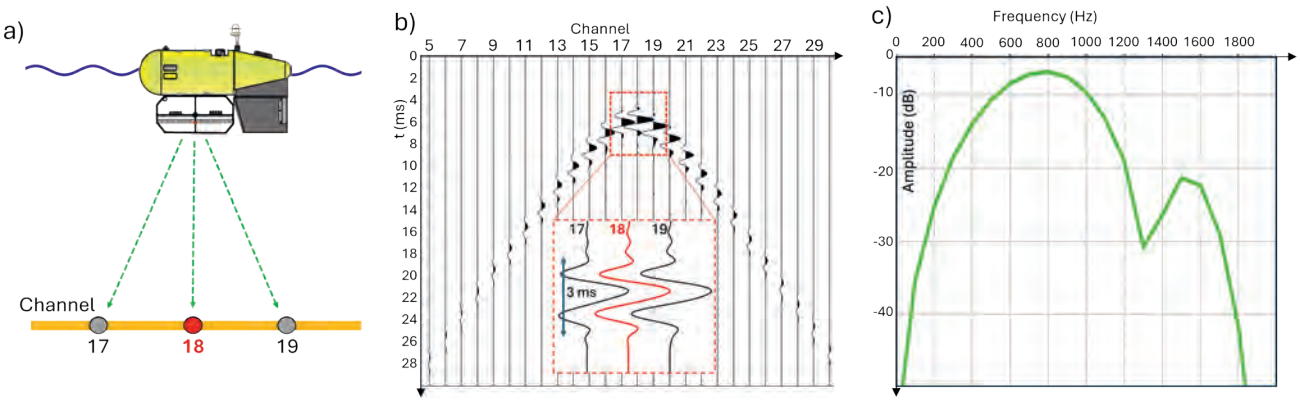

Figure 4 The direct seismic pulse from the sparker source (a) is recorded in the deep UHR streamer. The split-spread direct-wave recording is presented in (b) with a zoom of the central three pulses. In (c) the spectrum of the central pulse is displayed.

arranged in one single layer. The photo of the source in Figure 3 shows the aluminium frame with the 200 tips arranged in a 1 × 0.42 m rectangular pattern.

When the sparker is fired, a small bubble consisting of water vapour and plasma is formed at each of these tips, resulting in a downgoing acoustic wave in the water column. The torpedo-like yellow float keeps the frame with the 200 tips at a depth of ~0.6 m beneath the sea surface.

The source-over-streamer Novel configuration provided the opportunity to achieve an accurate source signature estimation, which was a requirement for a good de-signature processing of the data.

This source position is illustrated in Figure 4. In Figure 4a, the sparker source at a depth of ~0.6 m was located above the streamer towed at a depth of ~8 m where the downgoing seismic wave is recorded. Streamer channel 18 was located directly beneath the sparker source. Figure 4b shows the downgoing direct wave for 26 channels centred around channel 18. The zoom of the three central downgoing pulses shows a short-duration Ricker-like wavelet with a frequency spectrum shown in Figure 4c. This wavelet is a combination of the direct wave from the sparker tips and the reflections from the sea surface (i.e. the source ghost) and scattering from the sparker float above the sparker tips. In the frequency spectrum in Figure 4c we observe a notch at ~1250 Hz which was caused by the source ghost and corresponds to the source depth of 0.6 m. A favourable property of the sparker used in this field test is its short duration (~3 ms) and the absence of notches in the usable spectrum. Notches in the spectra of sparkers are caused by the bubble energy which is a well-known phenomenon in sparker sources and is caused by a second expansion of the initial expansive water vapour bubble (Kluesner et al., 2019). As shown in Kluesner et al (2019), conventional sparker sources with similar energy levels as in the SIG KappaSpark exhibit a much larger bubble lag, creating a long-duration source wavelet in the time domain and several notches in the spectrum which are a problem in the de-signature of the seismic data. In the SIG KappaSpark, the lag between the main peak and the bubble is so small that the first bubble notch occurs above the highest usable frequency in the data.

Another favourable property of the new sparker source is the lack of directivity of the source signature including the source ghost. In Figure 4b we observe that the wavelet for central channel 18 directly beneath the source is similar to the wavelets for its neighbouring channels 17 and 19 which have energy departing from the source at an angle of about 25 degrees from the vertical. Usually, we would expect a significant variation in the wavelet, mainly due to the tuning between the primary and the ghost. In this case we do not observe this, and we speculate that it may be caused by the scattering effect of the float carrying the sparker source.

This lack of directional diversity, the lack of bubble notches and the measurement of the downgoing vertical source wavelet (including its ghost) simplified the source de-signature and de-ghosting processes. In the processing workflow we used a single deconvolutional filter to de-signature, source de-ghost and shape the data to a desired spiky wavelet honouring the observed signal-to-noise (S/N) ratio.

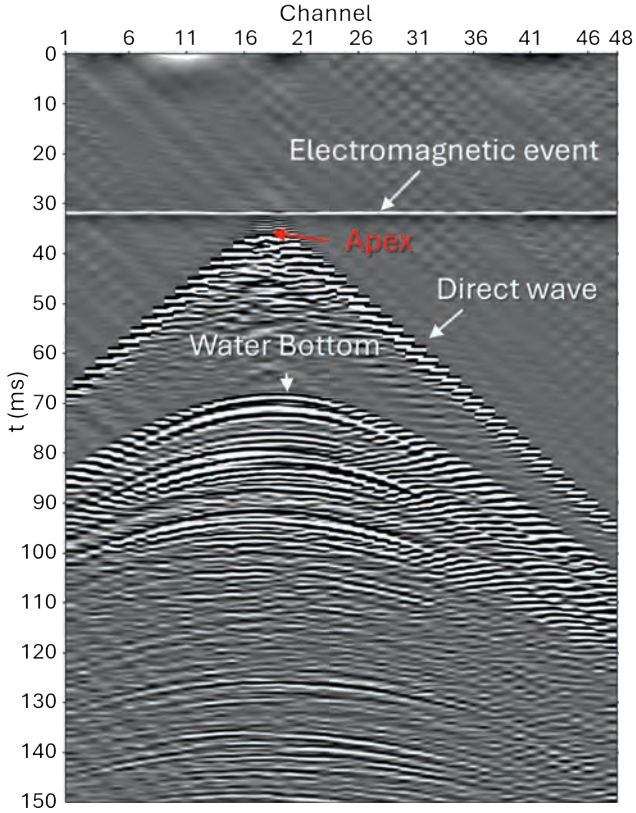

Figure 5 A shot gather with a firing problem, showing the direct wave, the water bottom reflection and the electromagnetic event used to correct the trigger error of the shot.

Correcting source timing and source/receiver positions

During QC of the field data, it was discovered that the firing time of the sparker source was out of sync with the instructed trigger time due to an unexpected extra charging time for the sparker capacitor. Mostly, the firing error was limited to less than a millisecond, but for some of the shots it was 30 ms or more. An example of this is shown in Figure 5 where a shot gather from the Novel survey is displayed. We can see the direct arrival and the water bottom reflection. However, we can also see that the apex of the direct wave in Channel 18 arrives at around 35 ms, which is not consistent with the vertical distance of around 7 m between the source and Channel 18. The direct traveltime for these 7 m in water should be around 5 ms. To correct the trigger error, we used a fortunate side-effect of the sparker source. When the sparker source was fired, the electromagnetic field surrounding it created a weak and almost simultaneous response in all the channels in the streamer. This was not caused by any acoustic wave in the water but was purely a response in the electronic systems in the streamer to the electromagnetic field in the water. This electromagnetic (EM) event is labelled in Figure 5.

The trigger error was corrected with the following three steps:

1. Stack the traces in each shot gather to create a single trace for each shot where the weak EM event will be enhanced and clearly visible.
2. From the stacked traces, select an 'anchor trace' with an estimated correct trigger time and measure the time lag of the electromagnetic event from all the other traces.
3. Shift all shot gathers to the anchor trace with the measured time lags.

Once the trigger error had been corrected, it was possible to accurately pick the first-break traveltime of the direct wave from the source to each of the channels. These traveltimes were used to derive the source-channel distance for each shot point using the water velocity of 1508 m/s which was found using a separate inversion process based on the direct arrivals. The distance from the source to the channel directly below (Channel 18) was measured along the entire sail-line. Channel 18 in the streamer was located vertically beneath the source as the sparker and streamer moved across the test line. It is reasonable to assume that the rapid variations in this source-to-channel distance observed along the sail line were caused by the up-and-down movement of the source due to sea waves and swells. We corrected for these rapid vertical wave-generated shifts in the source using a static shift which significantly reduced the jitter in the data, as shown in Figure 6.

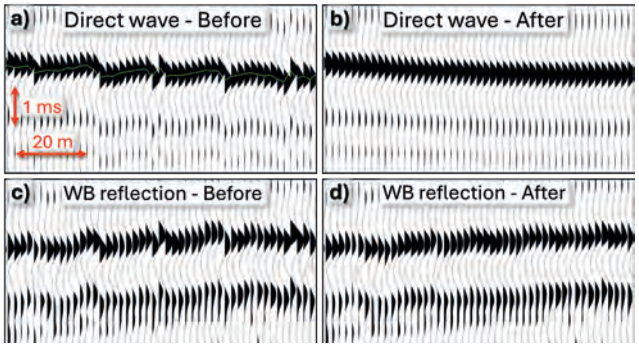

Figure 6 Common-channel (Ch 18) traces from the direct wave (a) and (b) and water bottom reflection (c) and (d) before and after correction of the source shifts due to wave motion.

Four zooms of a common channel gather for Channel 18 are displayed in Figure 6. About 85 m of the test line is shown in these zooms. Figures 6a and 6b show the direct wave before and after correction of the wave motion. We notice that a jitter of up to around 0.4 ms is observed in Figure 6a, which was corrected in Figure 6b by a static shift. This corresponds to a vertical movement of up to +/- 30 cm which is consistent with the wave height reported on the day of acquisition on 20 June, 2024 and illustrates the high level of accuracy required for the vertical source location on UHR surveys. After this correction, we show that the jitter had been removed on the direct wave (Figure 6b). Also, the jittering of the water bottom reflection was improved from before (Figure 6c) to after (Figure 6d) the correction. The water bottom reflection still contained noticeable lateral variations caused by the water bottom geology, as expected.

The remaining slowly varying source-to-channel distance was subsequently used to estimate the depth of the streamer, which was crucial in the receiver de-ghosting and imaging – see the discussion hereafter.

Designature and deghosting

We will now describe the solutions to two challenging problems inherent in UHR survey processing, (i) source deghosting and designature and (ii) receiver deghosting. The aim of these processing steps is to achieve a result with spiky, symmetrical reflectors with no remaining ghosts.

With the measurement of the direct wave in the Novel survey, as shown in Figure 4b, and the favourable lack of directionality of the sparker source, it was straightforward to create a 1D filter that performed the source deghosting, and shaped the data to a broadband, zero-phased, spiky wavelet taking into account the spectral S/N level. The shaping/source-deghosting filter was limited to frequency range with acceptable S/N levels, namely between ~150 Hz and ~1600 Hz. We refer to this process as *source designature*, as it removed the effect of the source wavelet and its ghost and shaped the wavelet.

The receiver deghosting, however, was potentially a more challenging problem to solve. Conventional UHR surveys typically lack accurate measurements of the streamer depth which is crucial for effective deghosting. In these cases, picking spectral notches in the data (Provenzano et al., 2020) is an option, but this may be challenging for noisy data. With the deep streamer in the Novel survey, the receiver ghosts (i.e. the downgoing sea-surface reflection of the seismic data) arrived as events that were completely separated from the upgoing primaries. This is clearly visible in Figure 7a, which shows the channel gather for Channel 18 before source designature and receiver deghosting.

All the subsurface reflectors in the data were ghosted, including the water bottom reflection indicated by the white arrow in Figure 7a. Its ghost (red arrow) arrived at around 10 ms after the water bottom primary reflection, which is consistent with the streamer depth of 8 m (2×8 = 16 m two-way vertical

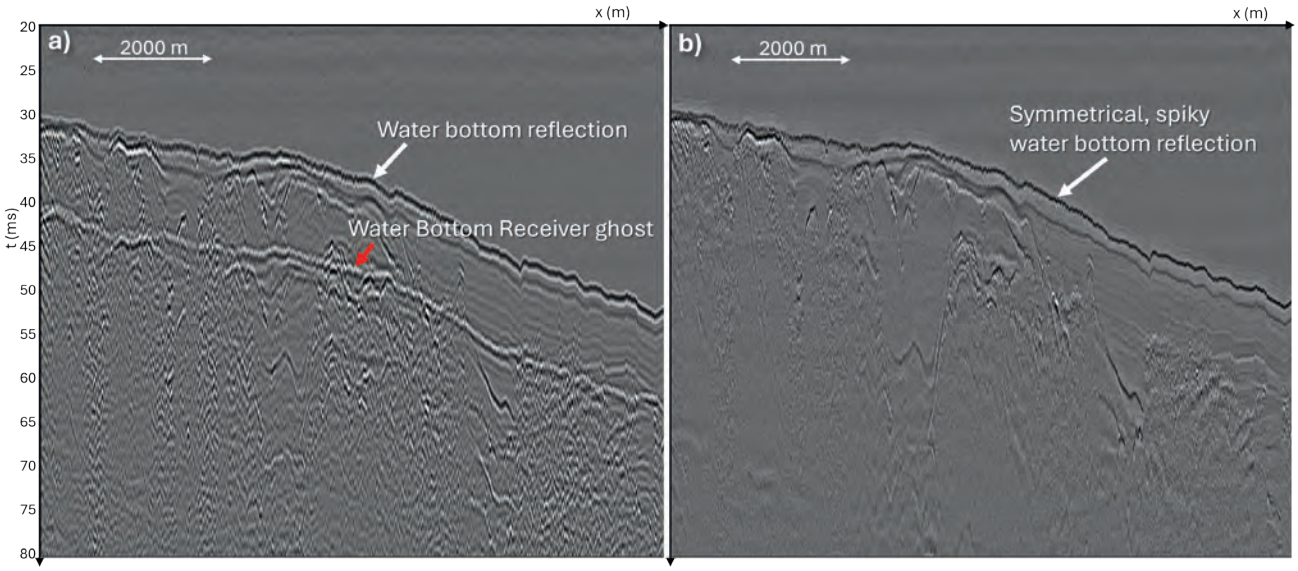

Figure 7 Common-channel (Channel 18) gather before (a) and after (b) source de-signature, source deghosting, spectral shaping and receiver deghosting.

distance divided by 1508 m/s water velocity). Figure 7b shows the common channel gather after the source designature and receiver deghosting. We first notice that the water bottom is spiky, with weak sidelobes and limited ringing, suggesting an accurate source designature.

The receiver ghost was modelled (Poole, 2013) using the corrected streamer depth from the Novel source-over-streamer setup and was adaptively subtracted from the data. The receiver ghosts were effectively attenuated and hardly visible in output, Figure 7b. However, there was still some remaining receiver ghost energy in the data as can be highlighted in Figure 8, which shows the frequency spectra before (green) and after (red) the source designature. The ripples in the spectrum with a period of ~100 Hz before the deghosting (green arrow) were suppressed, but still visible in part of the spectrum between 400 and 600 Hz after deghosting (red arrow). The receiver notches were suppressed further when longer-offset data with notch diversity was added and were not visible in the final image.

In Figure 8 we also observe that the spectrum has been widened, and that the source ghost notch at ~1250 Hz has been partly filled.

Comparison of images from novel and conventional survey geometries

We have described the unique processing steps for the Novel dataset which were facilitated by a source-over-streamer acquisition geometry and a new sparker source.

For the Conventional survey, with its shallow streamer towed behind the source, we did not have access to the direct downgoing wavelet, so it was more difficult to correct for vertical source motion and the exact streamer location. Apart from that, we applied the same processing steps for both surveys;

- Denoising
- Source trigger time correction – using the electromagnetic event
- Source wave-motion correction – using the direct wave in the Novel survey and the water bottom reflection in the Conventional survey
- Source designature – using the direct vertical wave extracted from the Novel survey
- Receiver deghosting
- Velocity model estimation – Using RMO gathers and 1508 m/s in the water column
- Tidal correction
- Kirchhoff depth migration and angle stack up to 36° – Image bin size 0.5 m

The observant reader will notice that de-multiple was omitted from the workflow. The reason for this was that the water bottom multiples appeared deeper than the shallow 30-40 m depth beneath the seabed that we focus on here.

The final migrated images of the ~10 km profiles are shown in Figure 9 with zooms of the smooth pockmark-free water bottom in the south-eastern part of the profile. The key geological features, as described above, are indicated by red arrows in Figure 9a, while the improvements in imaging from Conventional to Novel are shown by green arrows in Figure 9b. The main improvements brought by the source-over-deep-streamer Novel

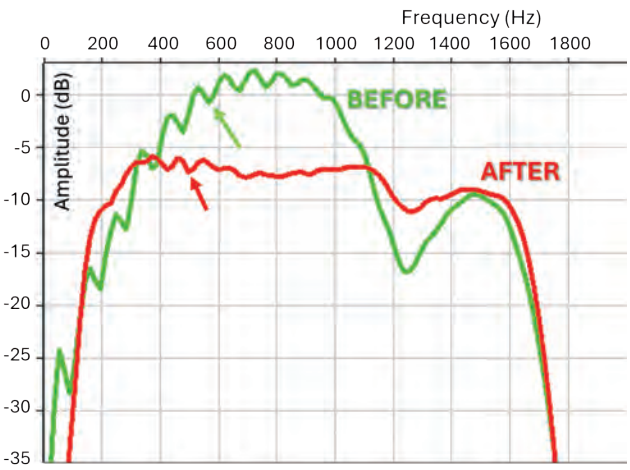

Figure 8 Common-channel (Ch 18) gather before (green) and after (red) source de-signature, source deghosting, spectral shaping and receiver deghosting.

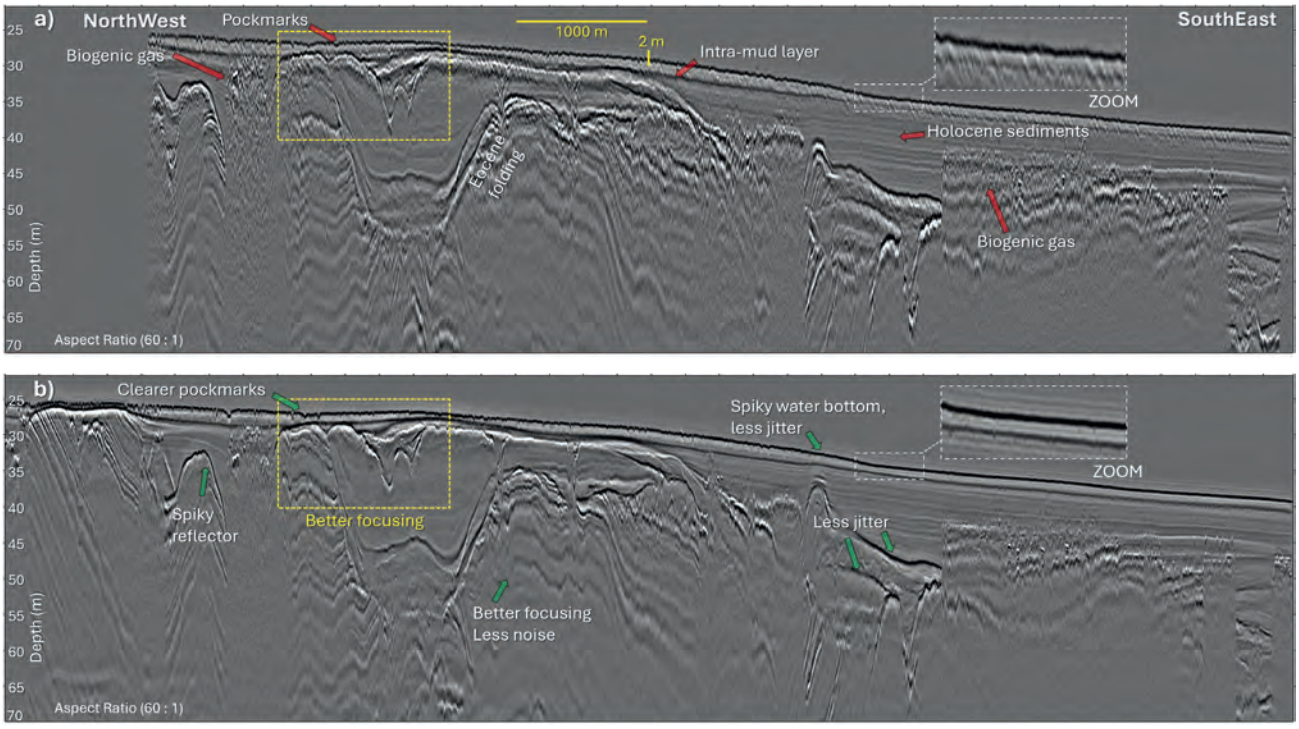

Figure 9 Final images from Conventional (a) and Novel (b) survey configurations with geological features indicated by the red arrows in (a) and improvements in imaging by green arrows in (b). The zoom of the smooth water bottom in the upper right-hand corner of (a) and (b) shows the false ripples introduced in the Conventional survey that have been suppressed by the Novel survey. The zooms in the yellow rectangles are shown in Figure 10.

survey configuration were better focusing, a reduction in jitter noise caused by the choppy water, and lower noise levels due to the deep streamer. The lack of wave-motion correction in the Conventional survey led to a broken-up water bottom and subsurface geology all along the profile. This is clearly visible in the zooms in Figure 10, with the Novel image showing improved focusing and less noise.

Part of the explanation for this overall improvement is due to the fact that there was more wind and waves (~60 cm wave heights) on June 19 2024 when the Conventional survey was acquired while the Novel survey, acquired on 20 June, had calmer weather (~30 cm wave heights). However, the main reason was the correction of the source shifts due to wave motion in the Novel survey combined with the greater position-stability and quieter conditions of the streamer at the ~8 m depth.

Conclusions

The only differences between the Novel source-over-streamer acquisition and the Conventional source-in-front-of-streamer acquisition described in this paper was the depth of the streamer and the location of the source relative to the streamer. The challenge of deghosting the deep streamer data from the Novel survey was solved by an accurate cable depth estimation and adaptive ghost model subtraction. The advantages of the Novel acquisition were clearly visible in the imaging examples with improved focusing, less jitter and less noise. The sparker source, used in both surveys, created a source wavelet of short duration, uniform directionality and no notches in the spectrum which is a great advantage in the source designature. With the Novel acquisition it was possible to measure the direct uninterrupted downgoing wave from the sparker source, which

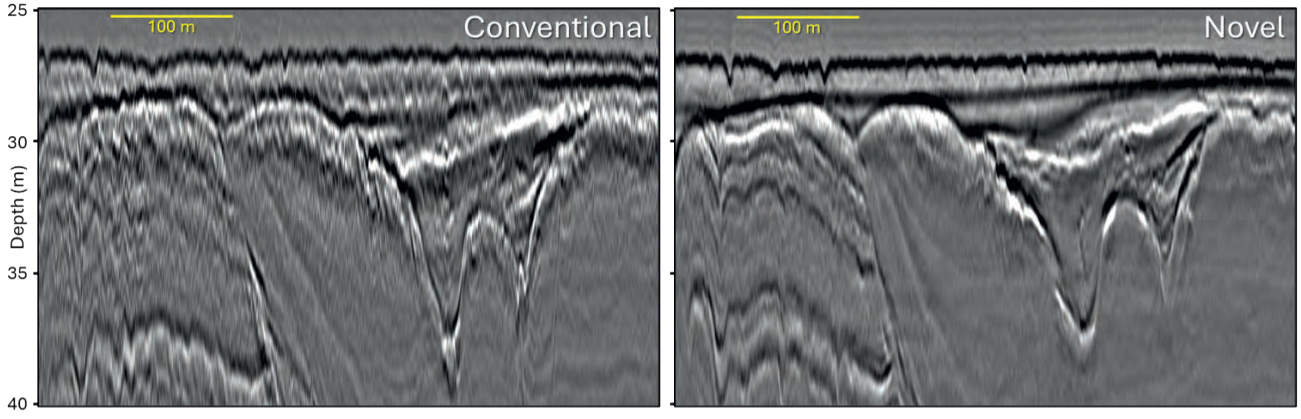

Figure 10 Zooms of the yellow rectangles from the Conventional and Novel surveys in Figure 9 with pockmarks, sedimentary layering and strong Eocene folding. The image improvement in the Novel survey is obvious.

was used for source designature, correcting for source wave motion and streamer depth corrections. The Novel acquisition also contained zero-offset and split-spread data which improves the usable fold and reduces NMO stretching. The combination of the Novel acquisition and the meticulous processing led to a significant reduction in noise and more detailed mapping of the geological features in the area, such as faults and folding, biogenic gas pockets, and thin bedding. Furthermore, the Novel acquisition with its deep streamer will be more robust in adverse weather conditions than the Conventional survey with its shallow streamer, reducing the need for downtime for future source-over-spread UHR acquisitions.

Acknowledgements

We thank our colleague Matt Ledger in Viridien for continuous expert advice on 2D UHR processing and for providing the velocity model. We would also like to thank the wider team of experts from TotalEnergies and Kappa for providing continuous support throughout the duration of the project from August 2024 to January 2025: Mourad Chiali, Eric Cauquil, Aldo Cardonna, Erwan Larvor, Natacha Barbier, Loic Nedelec, Fabrice Perreau and Sebastien Delecraz. Finally, we thank Kappa, SIG, TotalEnergies and Viridien for giving us permission to publish this paper.

References

Camerer, A., Grubb, C. and Mandroux, F. [2018]. Expanding the limits of operational feasibility in marine seismic acquisition: deploying a source-over-spread solution. 80th EAGE Annual Conference & Exhibition, *Extended Abstracts*.

Davies, D., Allinson, C. and Higson, M. [2020]. Obtaining sub-metre vertical and spatial resolution from seismic data – the Clair experience. EAGE 2020 Annual Conference & Exhibition Online, *Extended Abstracts*. https://doi.org/10.3997/2214-4609.202010456.

Dusart, J., Tarits, P., Fabre, M., Marsset, B., Jouet, G., Erhold, A., Riboulot, V. and Baltzer, A. [2022]. Characterization of gas-bearing sediments in coastal environment using geophysical and geotechnical data. *Near Surface Geophysics*, **20**, 478–493. https://doi.org/10.1002/nsg.12230.

Flamme, J., Tarits, P., Fabre, M., Jouet, G., Ehrhold, A., Lepot, A. and Marsset, B. [2020]. Characterization of shallow gas in coastal environment using jointly marine ERT and UHR seismic imaging. NSG2020 4th Applied Shallow Marine Geophysics Conference, *Extended Abstracts*. https://doi.org/10.3997/2214-4609.202020046.

Kluesner, J., Brothers, D., Hart, P., Miller, N. and Hatcher, G. [2018]. Practical approaches to maximizing the resolution of sparker seismic reflection data. *Marine Geophysical Research*, **40**, 279–301. https://doi.org/10.1007/s11001-018-9367-2.

Lebedeva-Ivanova, N., Polteau, S., Bellwald, B., Planke, S., Berndt, C. and Stokke, H.H. [2018]. Toward one-meter resolution in 3D seismic. *The Leading Edge,* **37**(11), 818–828, https://doi.org/10.1190/tle37110818.1.

Poole, G. [2013]. Pre-migration receiver deghosting and redatuming for variable depth streamer data. 83rd Annual International Meeting, SEG, *Expanded Abstracts*, 4216-4220.

Provenzano, G., Henstock, T.J., Bull, J.M. and Bayrakci, G. [2020]. Attenuation of receiver ghosts in variable-depth streamer high-resolution seismic reflection data. *Marine Geophysical Research*, **41**, article number 11. https://doi.org/10.1007/s11001-020-09407-9.

Telling, R., JafarGandomi, A. and Perratt, O. [2024]. Towards quantitative interpretation of UHR marine seismic: An example from the North Sea. 85th EAGE Annual Conference & Exhibition, *Extended Abstracts*. https://doi.org/10.3997/2214-4609.202410552.

Vinje, V., Lie, J.E., Danielsen, V., Dhelle, P.E., Siliqi, R., Nilsen, C.-I., Hicks, E. and Camerer, A. [2017]. Shooting over the seismic spread. *First Break*, **35**(6). https://doi.org/10.3997/1365-2397.35.6.89461.